Food Chemistry: X 25 (2025) 102073

Contents lists available at ScienceDirect

Food Chemistry: X

journal homepage: www.sciencedirect.com/journal/food-chemistry-x

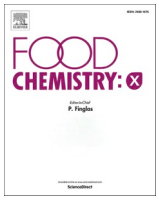

# Based on theoretical design simultaneous analysis of multiple neonicotinoid pesticides in beeswax by deep eutectic solvents extraction combined with UHPLC-MS/MS

Guodong Mu [a,1], Sha Yan [b,1], Fei Pan [a], Haitao Xu [a], Xu Jing [b], Xiaofeng Xue [a,*]

[a] State Key Laboratory of Resource Insects, Institute of Apiculture Research, Chinese Academy of Agricultural Sciences, Beijing 100093, China
[b] College of Food Science and Engineering, Shanxi Agricultural University, Taigu 030801, China

## ARTICLE INFO

*Chemical compounds studied in this article:*
Acetamiprid (Pubchem CID: 213021)
Clothianidin (Pubchem CID: 86287519)
Cycloxaprid (Pubchem CID: 45278274)
Dinotefuran (Pubchem CID: 135779803)
Flonicamid (Pubchem CID: 9834513)
Flupyradifurone (Pubchem CID: 16752772)
Imidacloprid (Pubchem CID: 86287518)
Imidaclothiz (Pubchem CID: 184601)
Nitenpyram (Pubchem CID: 3034287)
Sulfoxaflor (Pubchem CID: 16723172)
Thiacloprid (Pubchem CID: 115224)
Thiamethoxam (Pubchem CID: 5821911)
Proline (Pubchem CID: 145742)
alanine (Pubchem CID: 5950)
tetraethylammonium-chloride (Pubchem CID: 5946)
oxalic acid (Pubchem CID: 791)
tartaric acid (Pubchem CID: 875)
dichloroacetic acid (Pubchem CID: 6597)
citric acid (Pubchem CID: 311)
benzoic acid (Pubchem CID: 243)
malic acid (Pubchem CID: 525)
acetic acid (Pubchem CID: 176)
malonic acid (Pubchem CID: 867)
glycol (Pubchem CID: 174)
glycerol (Pubchem CID: 753)

*Keywords:*
Beeswax
Neonicotinoid pesticides
Deep eutectic solvent

## ABSTRACT

Beeswax, an FDA-approved component, has been extensively applied in feed, pharmaceutical, and food industries. The occurrence of neonicotinoid pesticides in beehive systems and their residues in beeswax have caused safety risks. Therefore, establishing a detection method for neonicotinoid pesticide residues in beeswax is crucial for ensuring its quality. The superhydrophobic property of beeswax makes it a challenge to develop suitable determination methods. In this work, we determined Proline and Oxalic acid as a suitable deep eutectic solvent (DES) to extract neonicotinoids from beeswax through theoretical design and verification tests. Systematic molecular dynamics simulations confirmed that hydrogen bonding and van der Waals forces facilitate the migration of neonicotinoid pesticides from beeswax into the DES. Performance analysis of the method revealed that the DES extraction combined with UHPLC-MS/MS approach exhibited excellent detection capabilities. It was applied to real beeswax sample analysis with the characteristics of simpleness, quickness, environmental friendliness, and high throughput.

*Abbreviations:* ANOVA, analysis of variance; COSMO-RS, conduct or-like screening model for real solvents; CTDC, Comprehensive Theoretical Dissolution Capacity; DES, deep eutectic solvent; DFT, density functional theory; DLLME, dispersive liquid-liquid microextraction; ESP, electrostatic potential; GAFF, General amber force field; GROMACS, GROningen MAchine for Chemical Simulations; HBA, hydrogen bond acceptor; HBD, hydrogen bond donor; IGMH, independent gradient model based on Hirshfeld partition; LINCS, linear constraint; LLME, liquid-liquid microextraction; LOD, limit of detection; LOQ, limit of quantification; MACCS, Molecular ACCess System; ME, matrix effect; MMFF94s, Merck Molecular Force Field 94 s; MRM, multiple reaction monitoring; PME, particle grid Ewald; RESP, restrained electrostatic potential; RSD, relative standard deviation; SMILES, simplified molecular input line entry system; STDC, Single Theoretical Dissolution Capacity; UHPLC-MS/MS, ultra high-performance liquid chromatography-tandem mass spectrometry; VMD, visual molecular dynamics; xTB, extended tight binding..

* Corresponding author.
*E-mail address:* xue_xiaofeng@126.com (X. Xue).
[1] Mu Guodong and Sha Yan contributed equally to this work.

https://doi.org/10.1016/j.fochx.2024.102073
Received 30 June 2024; Received in revised form 4 December 2024; Accepted 6 December 2024
Available online 7 December 2024

Conduct or-like screening model for real solvents
Molecular dynamics simulation
LC-MS/MS

## 1. Introduction

Beeswax, a kind of natural wax, is secreted from the wax glands of honeybees to build honeycombs (Hosseini et al., 2023). Various bee products, such as honey, bee pollen, and royal jelly, are stored in honeycombs (beeswax), thus the quality of beeswax plays an important role in ensuring honeybees' acceptance of foundation beeswax sheets and the quality of various bee products (Maia & Nunes, 2013). Due to its superhydrophobicity, plasticity, and non-toxicity, beeswax is a food and drug administration approved component and has been wildly applied in the feed industry, pharmaceutical industry, and food field (Brito-Pereira et al., 2023; Cheng et al., 2023). Beeswax-based edible films and coatings can be used as packaging materials to prolong the shelf-life of various fresh fruits (Hosseini et al., 2023). Beeswax-based edible oleogel can be used to produce fat substitutes or as a nutrient and medicine delivery system (Gao et al., 2021). Also, it can be used as a glazing agent and a color carrier as food additives (Giampieri et al., 2022).

The main compositions of beeswax include 27–40 % of monoesters, 11–28 % of hydrocarbons, 9–23 % of hydroxy monoesters, 7–16 % of diesters, 3–9 % of hydrocarbons, 1–18 % of free fatty acids, and others, with changes in proportions between species of honeybees (Giampieri et al., 2022). According to numerous reports, honeybees are under survival stress from pesticide exposure, and they are also carried back to the honeycomb by foragers (Bommuraj et al., 2019). Those persistent and highly hydrophobic pesticides can be diffused into the honeycomb system and accumulated in the beeswax (Lozano et al., 2019), which not only further contaminates other bee products, but also bring safety risks in the use of beeswax.

The occurrence of neonicotinoids in bee hive systems and its residue in beeswax have been widely reported (Murcia-Morales et al., 2022; Silvina et al., 2017; Tu & Chen, 2021). Neonicotinoids, a type of broad spectrum of efficacy insecticide, are the most extensively applied worldwide to control agricultural pests (Valverde et al., 2018). The toxic effect of neonicotinoids on pests is exerted by addressing the central nervous system (Silvina et al., 2017). Also, exposure to neonicotinoids can cause toxicity in people, such as anencephaly, autism spectrum disorders, memory loss, and so on (Yang et al., 2024). Considering the adverse influence and risk on human health, some regulations on neonicotinoids have been established. According to the World Health Organization and the Food and Agriculture Organization, 10–200 μg/kg body weight is set as the acceptable daily intake for acetamiprid, clothianidin, dinotefuran, imidaclothiz, nitenpyram, thiacloprid, and thiamethoxam. China gives the maximum residue limits of neonicotinoids in plant-derived foodstuffs (Yang et al., 2024). The residue limits of neonicotinoids in beeswax haven't been regulated, and the exposure of neonicotinoids through beeswax intake must be paid attention to with the increasing use of beeswax in the food and medicine fields. Additionally, because the contamination of neonicotinoids has adverse effects on colony health, the residue of evaluation of neonicotinoids in beeswax is crucial to monitoring honeybee population health and determining the cause of honeybee mortality (Bernardes et al., 2024).

Monitoring is vital to ensure the safety of beeswax with the acceptance of neonicotinoid residue. There have been some studies related to the establishment of a determination method for neonicotinoids in beeswax. Beeswax, the superhydrophobic matrix, is solid at room temperature and melts above 60 °C, which makes it a challenge to develop suitable determination methods (Tu & Chen, 2021). A large amount of organic solvent (acetonitrile) extraction is the traditional approach to preparing beeswax samples (Bommuraj et al., 2019), and it is time-consuming and not environmentally friendly. SPE and d-SPE were also used to prepare the neonicotinoids extract from beeswax (Jabot et al., 2015; Yáñez et al., 2013a; Yáñez et al., 2013b). During the above procedures, in addition to consuming large amounts of organic solvents, frequently additional clean-up was required. DESs, the combinations of specific solid substances (eq. choline chloride, organic acids, sugars) are alternative and emerging solvents (Cannavacciuolo et al., 2024). Due to their low toxicity, good biocompatibility, meeting the requirements of green chemistry, and high extraction performance, DES has been extensively applied in multi-type substance extraction from complex matrix, such as flavonoids from *Perilla frutescens* (L.) Britt. Leaves (Wang, Wang, et al., 2024; Wang, Zhang, et al., 2024), As (III) and Sb (III) ions from vegetable samples (Elik et al., 2024), organochlorine pesticides from water and apple juice samples (Tesfaye et al., 2023). For hydrophobic matrices, such as edible oils, Ju et al. developed dispersive liquid-liquid microextraction (DLLME) based on DES combined with HPLC-DAD to determine thiamethoxam, imidacloprid, and thiacloprid (Ju et al., 2023).

In the present study, to develop a simple, quick, green, high efficiency, and high-throughput method to analyze the neonicotinoids from beeswax, a based on DES extraction combined with UHPLC-MS/MS analysis approach would be established. The specific process was as follows: 1) based on theoretical design screen suitable DES combinations; 2) actual experiment verification and optimization of extraction process; 3) the interpretation of extraction mechanism; 4) the evaluation of method performance; 5) comparison of DES with other extraction methods; 6) actual beeswax sample analysis. This work helps control the quality of beeswax and provides an application potential of DES to the superhydrophobic matrix.

## 2. Materials and methods

### 2.1. Materials and reagents

Beeswax samples were collected from hives and purchased from a local market (Table S1). Twelve neonicotinoid pesticides, including acetamiprid (ACE, 99 %), clothianidin (CLO, 99 %), cycloxaprid (CYP, 99 %), dinotefuran (DIN, 98 %), flonicamid (FLO, 99 %), flupyradifurone (FLU, 98 %), imidacloprid (IMI, 99 %), imidaclothiz (IMZ, 98 %), nitenpyram (NIT, 97 %), sulfoxaflor (SUL, 98 %), thiamethoxam (THX, 98 %), thiacloprid (THI, 98 %), were purchased from Macklin Biochemical Co., Ltd. (Shanghai, China).

Proline (Pro, 98 %), alanine (Ala, 98 %), and tetraethylammonium-chloride (TEAC, 98 %), as hydrogen bond acceptors (HBAs), were purchased from Macklin Biochemical Co., Ltd. (Shanghai, China). And oxalic acid (OxA, 99 %), tartaric acid (TA, 95 %), dichloroacetic acid (DclA, 98 %), citric acid (CtA, 98 %), benzoic acid (BzA, 99 %), malic acid (MA, 98 %), acetic acid (AC, 99 %), malonic acid (MLA, 98 %), glycol (Gol, 99.5 %), glycerol (Gly, 99 %), as hydrogen bond donors (HBDs), were purchased from Shanghai Aladdin Biochemical Technology Co., Ltd. (Shanghai, China). HPLC-grade acetonitrile and methanol were purchased from Thermo Fisher Scientific (Waltham, Massachusetts, USA). The ultrapure water was prepared by the Milli-Q water purification system (Millipore, Billerica, USA).

### 2.2. Preparation of DESs

An HBA and an HBD were mixed with a molar ratio of 1:1 at 80 °C

until the solution was homogenous and transparent. When it was cooled at room temperature and its liquid state remained, the DES was successfully formed for further analysis.

### 2.3. COSMO-RS simulation screening

Firstly, it is necessary to optimize the geometric structure and charge density of each target molecule in the system using density functional theory (DFT). In this study, molecular optimization was performed using the COSMO-BP-TZVP template in TmoleX19 software (Beijing Tech-Box S&T Co. Ltd., Beijing, China). The template includes the def-TZVP basis set, DFT at the BP-86 functional theory level, and conduct or-like screening model for real solvents (COSMO-RS). All COSMO-RS calculations were conducted using the COSMOthermX18 software (Beijing Tech-Box S&T Co. Ltd., Beijing, China) with the BP_TZVP_18.ctd parametrization. Because COSMO-RS is not suitable for ion calculations, the quaternary ammonium salts, as HBAs were treated as ion pairs in this study and optimized by TmoleX19 software (Wojeicchowski et al., 2020).

The extraction yield of each neonicotinoid pesticide is proportional to its solubility in the solvent. The COSMOthermX18 software can characterize the relative solubility of each compound. The relative solubility values were calculated under the condition of infinite dilution (non-iterative). In this work, COSMO-RS was used to predict the relative solubilities of 12 neonicotinoid pesticides in 473 DESs at 75 °C and infinite dilution conditions. The HBA and HBD of each DES were present in an equal molar ratio. The relative solubility was calculated according to the eq. (1):

$$lgX_i = lg\{exp[(\mu_i^P - \mu_i^S)/RT]\} \quad (1)$$

where $X_i$ represents solute relative solubility, and $\mu_i^P$ and $\mu_i^S$ are the chemical potentials of the pure solute, i.e., neonicotinoid pesticide and the pure solute at infinite dilution of the solvent (Wang, Wang, et al., 2024; Wang, Zhang, et al., 2024).

### 2.4. Evaluation of the overall dissolution ability of each DES to all neonicotinoids

To comprehensively assess the overall dissolution ability of each DES to all neonicotinoids, the log10 (x_RS) value of each neonicotinoid in DES was normalized, resulting in a Single Theoretical Dissolution Capacity (STDC) ranging from 0 to 1. Subsequently, the STDC values for all neonicotinoids were summed and averaged to obtain the Comprehensive Theoretical Dissolution Capacity (CTDC), as shown in eq. (2–3). The CTDC value ranges from 0 to 1, where a higher CTDC value indicates a stronger overall dissolution ability of DES towards neonicotinoids, while a lower CTDC value suggests a weaker overall dissolution ability.

$$STDC = \frac{log_{10}(x\_RS) - Min(log_{10}(x\_RS))}{Max(log_{10}(x\_RS)) - Min(log_{10}(x\_RS))} \quad (2)$$

$$CTDC = \frac{\sum_{k=1}^{n} STDC_k}{n} \quad (3)$$

where Min ($log_{10}$ (x_RS)) and Max ($log_{10}$ (x_RS)) represent the minimum and maximum $log_{10}$ (x_RS) values, respectively. n represents the number of neonicotinoid pesticides.

### 2.5. Sample preparation and extraction procedure

According to the reference (Tu et al., 2024) with some modifications, we initially spiked the blank beeswax sample with neonicotinoid pesticides. 5.0 g of beeswax was added into a tube, and the tube was in a 75 °C water bath for 10 min to melt the beeswax. Subsequently, 100 μL of standard solution (5 mg/L) was added to the melted beeswax. After fully mixed, these beeswax samples spiked with neonicotinoids were stored at 4 °C for further analysis.

During the liquid-liquid microextraction (LLME) process, 1 mL of DES was added to 5.0 g of melted beeswax and vortexed in a 75 °C water bath for 15 min. Subsequently, the tube was left in the water bath for 2 min to accomplish phase separation. 200 μL lower DES phase was collected and diluted to 1.0 mL with MeOH-H2O (1:1, *v*/v). Finally, the dilution was passed through a 0.22 μm PTFE filter for UHPLC-MS/MS analysis.

### 2.6. Molecular dynamics simulation

#### 2.6.1. Molecular fingerprint calculation

The simplified molecular input line entry system (SMILES) of 12 neonicotinoid pesticides were calculated using the RDKit tool, and subsequently, their Molecular ACCess System (MACCS) molecular fingerprints comprising 166 unique molecular features were computed (Bento et al., 2020). MACCS molecular fingerprints are defined based on the presence or absence of specific substructures in the molecule, wherein each feature corresponds to a distinct chemical substructure (Xu et al., 2022). Finally, we employed the Tanimoto similarity calculation method to assess the similarity of MACCS molecular fingerprints among pairwise compounds.

#### 2.6.2. Structure optimization

A biphasic system comprising beeswax and DES was constructed to explore the extraction mechanism of neonicotinoid pesticides from beeswax using DES. Myrieyl palmitate, which is the primary constituent of beeswax, was selected to represent the beeswax phase. The DES consisted of Pro and OxA, and IMI served as the representative molecule for neonicotinoid pesticides. The above-mentioned molecular structures were generated using the Avogadro program (Hanwell et al., 2012) and pre-optimized with the Merck Molecular Force Field 94 s (MMFF94s) to rectify unreasonable bond lengths and angles. Based on the ORCA program in the quantum chemistry, geometry optimization, and vibration analysis of small molecules were performed using the r2SCAN-3c method (Neese, 2018), while single-point energy calculations were employed the B3LYP/G D3 def2-TZVP method with def2/J as an auxiliary basis set. After the single-point energy was calculated, Restrained electrostatic potential (RESP) charges were computed using the Multiwfn program for wave function analysis (Lu & Chen, 2012).

#### 2.6.3. Molecular dynamics simulation of beeswax phase

A 15 × 15 × 10 nm simulation system containing 157 myristyl palmitate molecules and 40 IMI molecules was constructed. Molecular dynamics simulations were conducted using the Groningen machine for chemical simulations (GROMACS) program (Abraham et al., 2015), with the amber14sb force field and TIP3P employed to construct the water model. The small molecule topology was calculated by the General amber force field (GAFF), and the pairs of ions were introduced to maintain electrical neutrality. The energy minimization process began with the application of the steepest descent method (1000.0 kJ/mol/nm), followed by subsequent energy minimization using the conjugate gradient method (100.0 kJ/mol/nm). The system was subsequently pre-balanced with 1 ns of NVT and 1 ns of NPT. After the pre-equilibration finished, a 10 ns production simulation was conducted to obtain the stabilized beeswax phase containing IMI. All bonds involving hydrogen atoms are constrained using the default linear constraint solver (LINCS) algorithm. The simulated temperature (298.15 K) and pressure (1.0 bar) were controlled using a V-rescale thermostat and a Parrinello-Rahman pressure coupling method with time constants of 0.1 and 2 ps, respectively. The long-range interactions were evaluated using the particle grid Ewald (PME) method, while the Van der Waals interactions were calculated with a cut-off distance of 10 Å.

#### 2.6.4. Beeswax-DES biphasic molecular dynamics simulation

To indicate the molecular dynamics process, a new box-like model was built. The dimensions of the new box in the x and y directions remained unchanged, while the positive and negative sides of the z-axis were extended by 5 nm each, resulting in a final box size of 6.9 × 6.9 × 14.59 nm. The molecular coordinates of the balanced beeswax phase containing IMI were inserted into the new simulation box and centered. Subsequently, 630 DES combinations (Pro: OxA = 1: 1) and 5041 water molecules were introduced into the system. Molecular dynamics simulations of the biphasic system were conducted for a duration of 500 ns under isovolumetric conditions with a time step of 2 fs, and snapshots were collected every 100 ps. Other parameters were consistent with the previous research (Pan et al., 2023).

#### 2.6.5. Noncovalent adsorption simulation

The IMI molecules in the DES phase, with their neighboring DES molecules within a distance of 5 Å, were isolated from the beeswax-DES biphasic molecular dynamics simulations. Subsequently, these IMI molecules underwent geometric optimization at the GFN2 level (Bannwarth et al., 2019) by the extended tight binding (xTB) program (Bannwarth et al., 2021). Further, the independent gradient model based on Hirshfeld partition (IGMH) method was employed to visualize the interaction between DES and IMI molecules. IGMH is characterized as utilizing Hirshfeld molecular density partitioning to mitigate misinterpretation of interaction nature and enhance precision in the physical interpretation of IGMH, which revealed a significant advancement over the IGMH method (Lefebvre et al., 2017). Through wave function analysis, IGMH can determine the interaction contributions between atoms and atom pairs. The three-dimensional function δg was utilized to visualize the interaction regions among atoms. The calculations and visual analysis were performed using Multiwfn 3.8 (dev) program and visual molecular dynamics (VMD) 1.9.3 software (Lu & Chen, 2012).

In IGMH analysis, δg in the system, as a 3D real space function, represented the interactions among all atoms, and the larger values indicated the stronger interatomic interactions. Furthermore, δg can be divided into two components: $\delta g^{intra}$ representing intra-segment interactions and $\delta g^{inter}$ denoting inter-segment interactions. The calculation of $\delta g^{inter}$ between multiple segments follows Eq. (4–6) provided below, where *A* denotes the number of segments (Lu & Chen, 2012).

$$g^{inter}(r) = |\sum_{A}\sum_{i\in A}\nabla\rho_i(r)| \tag{4}$$

$$g^{IGMinter}(r) = |\sum_{A} abs\left[\sum_{i\in A}\nabla\rho_i(r)\right]| \tag{5}$$

$$\delta g^{inter}(r) = g^{IGM,inter}(r) - g^{inter}(r) \tag{6}$$

### 2.7. Optimization of DES extraction conditions

In this part, the extraction conditions of DES, including the molar ratio of HBA and HBD, the addition of water, extraction time and the volume of DES, were optimized by single factor experiment, and the basic conditions were as follows: the molar ratio of Pro to OxA was 1:1, 20 % of water, 3 min of extraction time, and 1000 μL of DES volume. The molar ratio of Pro to OxA was set as 3:1, 2:1, 1:1, 1:2, and 1:3; the water content increased from 20 % to 100 %; the extraction time was adjusted to 3 min, 6 min, 9 min, 12 min, 15 min, and 18 min; the addition of DES volume ranged from 500 μL to 1750 μL. Under the above-mentioned conditions, the extraction efficiencies of neonicotinoid pesticides were evaluated, respectively.

### 2.8. UHPLC-MS/MS analysis

A 1290 series UHPLC system and a 6495 tandem mass spectrometer (Agilent, Palo Alto, CA, USA) were used to quantify Neonicotinoid pesticide residues in beeswax. An EclipsePlus C18 RRHD (Agilent, 3.0 × 150 mm, 1.8 μm) was as a separated column. The mobile phases consisted of 0.1 % formic acid in water (A) and acetonitrile (B). The gradient elution program was 0 min: 5 % B; 3 min: 30 % B; 8 min: 90 % B; 9 min: 90 % B; 9.01 min: 5 % B; 12 min: 5 % B. The flow rate was 0.3 mL/min. MS parameters were AJS ESI used as the ion source, 11.0 L/min of drying gas flow, 250 °C drying gas temperature, 12.0 L/min of sheath gas flow, and 350 °C sheath gas temperature. Table 1 outlines the optimized multiple reaction monitoring (MRM) parameters.

### 2.9. Validation of method performance

According to SANTE 11,312/2021, the method validation was evaluated based on matrix effect (ME), linearity, limit of quantification (LOQ), limit of detection (LOD), mean recovery, repeatability, and reproducibility. The calculation equation of ME was according to the description of the reference (Erminia Schiano et al., 2024). The ME ranges from 80 % to 120 %, which indicates that ME is negligible. For the linearity, the matrix-matched calibration curves and solvent calibration curves were prepared at seven concentration levels (0.1 μg/L, 1 μg/L, 5 μg/L, 10 μg/L, 50 μg/L, 100 μg/L, 500 μg/L). The lowest spiked concentrations with a chromatographic peak at a signal-to-noise of 3 and 10 were determined as LOD value and LOQ value, respectively. The recoveries and repeatabilities of this method were calculated by determining blank matrix samples at three concentrations with six independent replicates. The reproducibilities were tested on three consecutive days covering different solvents, reagents, and blank material.

### 2.10. Data processing

The data from DES-LLME optimization experiments were analyzed via one-way analysis of variance (ANOVA) and Duncan pairwise comparisons test. All statistical analyses in this study were performed using GraphPad Prism 9 software (GraphPad Software, USA). The significance level was defined as 0.05.

## 3. Results and discussion

### 3.1. Based on theory design to screen DES by COSMO-RS

In this work, COSMO-RS was used to screen optimal DES combinations by predicting the solubility of neonicotinoid pesticides in various DESs. Based on previous reports involving multiple types of DES combinations, we chose 11 kinds of HBAs (Table S2) and 43 kinds of HBDs (Table S3) to form DESs and evaluate their solubilities.

A suitable DES should have high extraction performances for all neonicotinoids. To evaluate the CTDC of each DES towards 12 kinds of neonicotinoids, we calculated CTDC values based on $\log_{10}$ (x_RS) values of all potential DES combinations. The predicted results were illustrated

**Table 1**
Multi-reaction monitoring parameters of 12 neonicotinoid pesticides.

| Analytes | RT (min) | Parent ion (*m/z*) | Product ion (m/z) | CE (volt) |
|---|---|---|---|---|
| ACE | 6.87 | 222.9 | 126.0*,99.1 | 15,18 |
| CLO | 6.52 | 249.9 | 169.0*,131.9 | 12,17 |
| CYP | 6.15 | 323.4 | 276.1151.1* | 17,22 |
| DIN | 4.86 | 203.3 | 129.1*,114.0 | 5,10 |
| FLO | 6.27 | 230.3 | 203.3174.1* | 20,25 |
| FLU | 7.19 | 289.4 | 126.0*,90.1 | 20,35 |
| IMI | 6.73 | 256.0 | 208.9*,175.0 | 12,16 |
| IMZ | 6.91 | 262.1 | 181.1*,122.1 | 15,27 |
| NIT | 5.30 | 271.0 | 237.0,56.0* | 6,26 |
| SUL | 7.45 | 278.3 | 174.2*,154.2 | 10,25 |
| THI | 7.37 | 253.0 | 186.1126.1* | 12,15 |
| THX | 6.07 | 291.9 | 210.9*,180.9 | 10,22 |

* Quantitative ion.

as a heat map (Fig. 1). In the heap map, different colors indicated the relative solubilities for 12 neonicotinoid pesticides in different DESs at 75 °C. Bright colors represent high dissolving capacity, while dark colors represent low dissolving capacity. According to the CTDC values, Pro-OxA, Ala-OxA, Pro-MLA, Pro-MA, Pro-TA, TEAC-CtA, Pro-DclA, Gly-OxA, Pro-CtA, TEAC-BzA, Pro-MlA, TEAC-AC, Pro-BzA, Ala-DclA, TEAC-Gol and TEAC-Gly had higher theoretical dissolution capacities for neonicotinoid pesticides, making them potential DES combinations for verification tests.

### 3.2. Verification of DES combinations

To further determine the most suitable DES combination based on the COSMO-RS prediction results, the 16 DESs were used to extract neonicotinoid pesticides from beeswax at 75 °C. In the actual preparation process, four of the theoretical DESs with high melting points condensed into a solid state at room temperature. Therefore, twelve DESs (Fig. S1A) were successfully synthesized to verify their extraction performances. Although neonicotinoid pesticides are a type of heterocyclic compound containing nitrogen, due to the differences in substituents, each neonicotinoid pesticide exhibits unique physical and chemical properties, such as the solubilities in different DESs. Comprehensive consideration revealed that Pro-OxA and Ala-OxA indicated better extraction performances for all twelve neonicotinoid pesticides compared to other DES combinations (Fig. S1B). Among these target neonicotinoids, DIN, THX, NIT, IMZ, and IMI were more easily extracted by Pro-OxA, while CLO and FLU revealed lower recovery rates. Thus, DES extraction conditions need to be further optimized to improve the extraction efficiency.

### 3.3. Optimization of extraction process

We optimized the main conditions, including the molar ratio of HBA and HBD, water content, extraction time, and the volume of DES, to improve the extraction performance of neonicotinoid pesticides.

The molar ratio of Pro to OxA: When the molar ratio of HBA to HBD was 3:1 or 2:1, the DESs could not be synthesized. The effect of the molar ratio of HBA to HBD on the extraction efficiencies of neonicotinoid pesticides is shown in Fig. S2A. The total amounts of neonicotinoid pesticides extracted by the DES significantly decreased with the increase in the proportion of HBA, which may be attributed to the increase in viscosity.

The addition of water: A large number of hydrogen bonds between DESs and target components can lead to high viscosity and low fluidity of synthetic DES (Gutiérrez et al., 2021). The addition of water into the DES system is effective in decreasing the viscosity of DES. However, excess water can disrupt the balance between DES and target compounds and have an adverse effect on the extraction efficiency. When the addition of water increased from 20 % to 30 %, the recovery rates of neonicotinoid pesticides increased. However, the continuous addition of water had a negative effect on the extraction effect (Fig. S2B). Moderate water content was beneficial for improving the dispersion of DES in the beeswax sample. As the water content increased, it destroyed the hydrogen bond structure within the DES and weakened the interaction between the targets and the DES (Huang et al., 2017; Sapir & Harries, 2020). Thus, a 30 % water content in DES was determined.

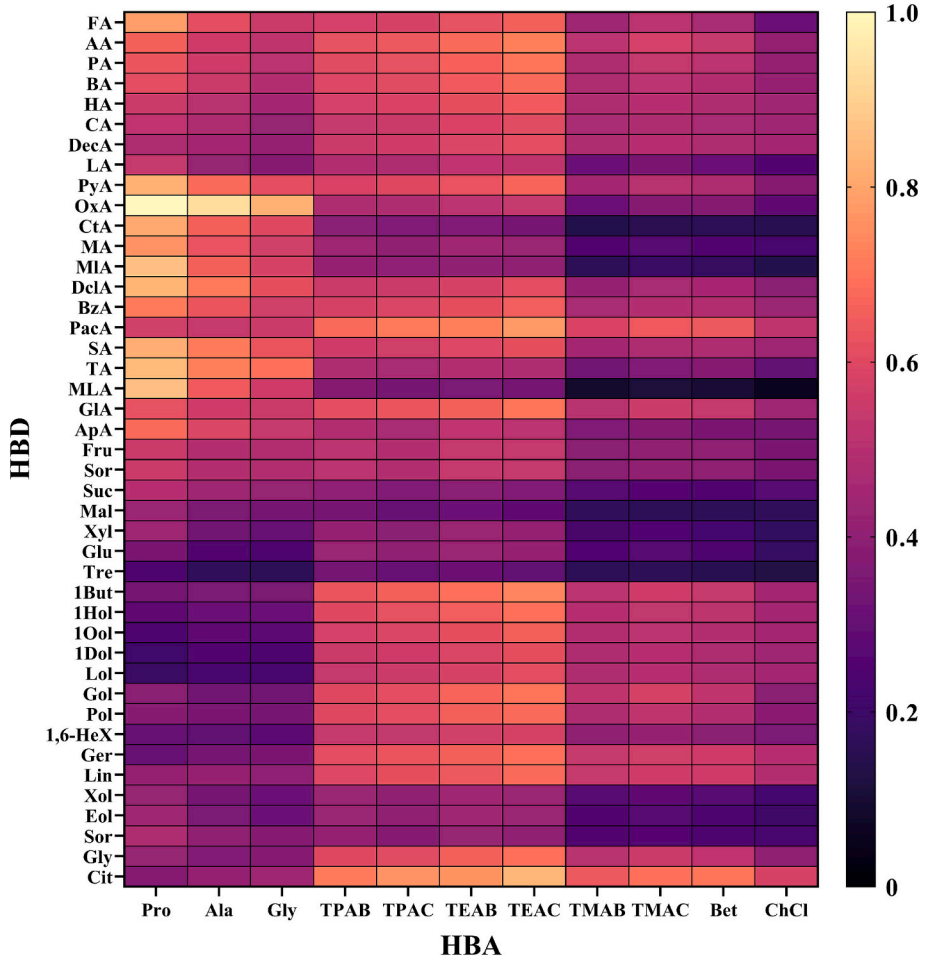


**Fig. 1.** Heat map of Comprehensive Theoretical Dissolution Capacity in 473 DES (HBA: HBD = 1: 1) at 75 °C using COSMO-RS.

Extraction time: A dynamic equilibrium can be obtained as the extraction progresses, and the extraction time influences the extraction amount until adsorption equilibrium is reached. Extending the extraction process not only consumes time but also leads to the extraction of more impurities, which interferes with the analysis results (Zhang et al., 2024). As Fig. S2C shows, when the extraction time was 15 min, the recovery rates reached peak values, so 15 min was selected as the optimal extraction time.

The volume of DES: A moderate addition of DES can promote the transport of neonicotinoid pesticides from beeswax to the DES layer, while excess DES can cause dilution. The extraction amount to most neonicotinoid pesticides enhanced with the increase of the volume of DES varied from 500 μL to 1000 μL and the recovery rates decreased with continuous increases of the volume of DES (Fig. S2D).

According to the optimized design, the optimal extraction conditions were determined as follows: a deep eutectic solvent (Pro-OxA) was prepared with a molar ratio of 1:1 and water content of 30 %. A volume of 1000 μL of the prepared DES was added to 5 g of beeswax, followed by shaking extraction in a water bath at 75 °C for 15 min. Under these optimized conditions, the recovery rates of 12 neonicotinoids ranged from 79.7 % to 103.5 %, with relative standard deviations (RSDs) ranging from 0.86 % to 6.07 %.

### 3.4. Interpretation of extraction mechanism

To interpret the extraction mechanism of neonicotinoids by DES, a representative neonicotinoid pesticide was selected based on MACCS fingerprint similarity. The MACCS fingerprint derives from key substructural features, encompassing a wide range of atomic properties, various chemical bond topologies, and characteristics of atomic neighborhoods, allowing for a comprehensive comparison of overall similarity between different compounds (Bento et al., 2020). The heat map of pairwise similarity scores for neonicotinoid pesticides, obtained using the Tanimoto method, revealed a high degree of fingerprint similarity among most neonicotinoid pesticides (Fig. 2A). This high similarity suggests that these pesticides may possess similar physical properties (Yang et al., 2022). Among the 12 neonicotinoid pesticides, the average fingerprint similarity score of seven targets, including DIN, NIT, THX, CLO, IMI, IMZ, and CYP, was 0.7833. Comparing the fingerprint similarity of each neonicotinoid pesticide, IMI had the highest average similarity score of 0.7052, followed by IMZ (0.6916) and THX (0.6913) (Fig. 2B) (Maggiora, 2014). According to the similar property principle, chemical molecules with similar fingerprints indicate similar biological activities or physicochemical properties. Therefore, we chose IMI as a representative of neonicotinoid pesticides for subsequent mechanism studies.

Molecular electrostatic potential (ESP) is a widely employed and pivotal approach for elucidating the reaction behavior of molecules. The nucleophilic moiety of each molecule exhibits favorable interactions with the regions containing the highest positive potential in another molecule, which provides intuitive insights into the structure, properties, and behavioral characteristics of chemical molecules (Politzer & Murray, 2021). Fig. 2C shows the ESP maps of the main substances in the molecular dynamics simulation system. Myricyl palmitate, the predominant component in beeswax, has ester moieties highlighted in blue, which indicates that the electrostatic potential values of these regions are positive and these regions are more electrophilic. In addition, the structure of myricyl palmitate molecular comprises a significant number of hydrophobic alkanes, resulting in weak electrostatic potential values in these regions. The carboxyl position of Pro and OxA demonstrates strong electrophilicity, and the intermediate region displays nucleophilic characteristics. Their structures are beneficial to facilitate interaction with IMI (Cons et al., 2022), and compete with the neonicotinoid molecules from a superhydrophobic environment.

To further explain the DES extraction mechanism, we constructed a biphasic molecular dynamics simulation system comprising the beeswax

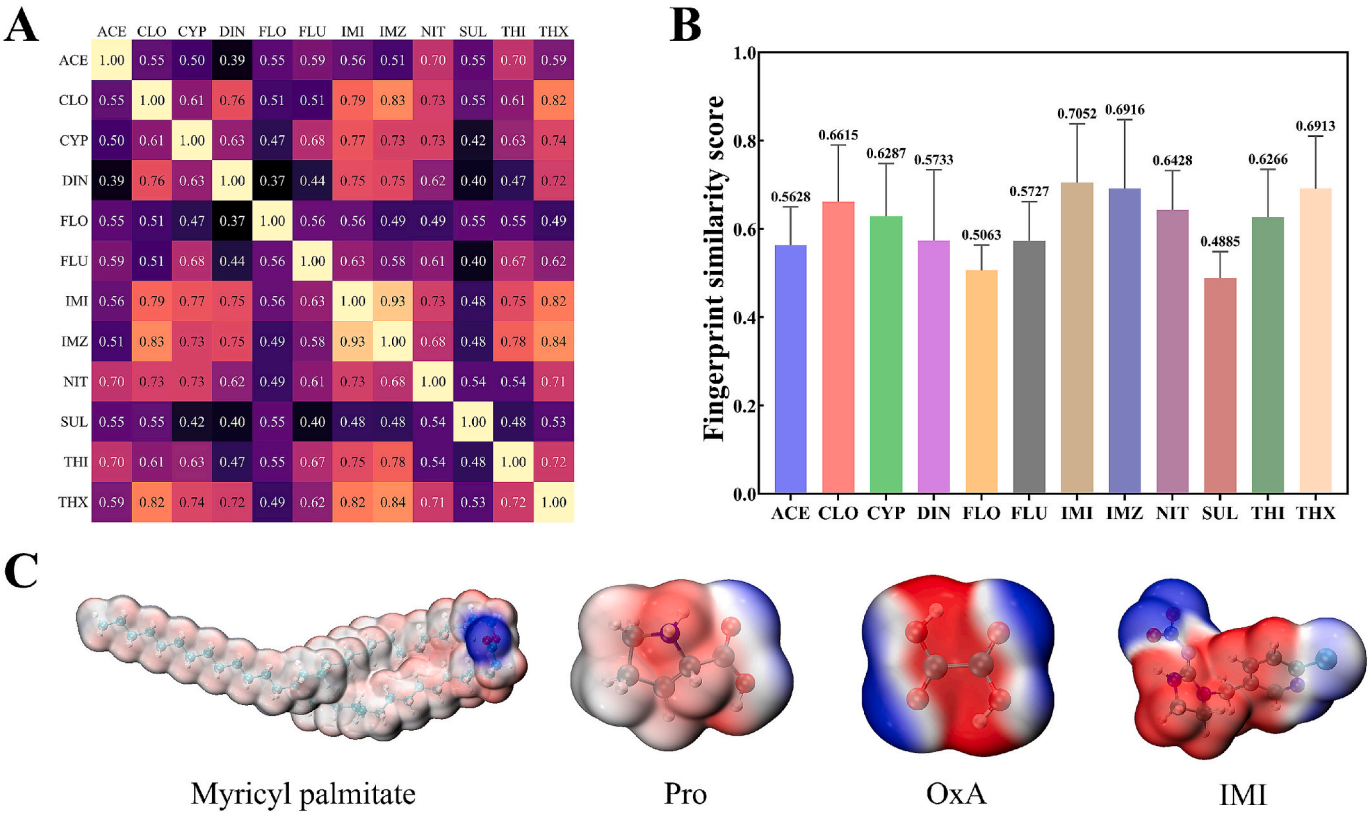


**Fig. 2.** The similarity results of MACCS molecular fingerprints calculated by the Tanimoto method. (A) Heat map of two-by-two similarity between compounds, (B) Average similarity score of each compound to other compounds, (C) Electrostatic potential maps of major molecules for molecular dynamics simulations.

layer and DES layer and performed a 500 ns molecular dynamics simulation. The initial state of the simulation system is shown in Fig. 3A. The density distribution of different representative molecules along the *Z*-axis revealed strong hydrophobicity of the beeswax matrix (Fig. 3B). During the process of the 500 ns simulation, IMI gradually transferred from the beeswax layer into the DES layer (Fig. 3C). Compared to the initial density distributions of IMI in the beeswax layer (Z-axis: 4–10 nm), it was decreased (Z-axis: 3–5 nm) along with IMI migrating to the two-phase interface region (Fig. 3D). At the end of the simulation, there was a significant reduction in the IMI density of the beeswax layer, while its concentration greatly increased in the DES layer (Fig. 3E). Thus, the synthetic DES was a suitable extraction solvent for IMI in beeswax.

To elucidate the complex interplay between IMI and the DES, we quantified the number of hydrogen bonds formed between IMI and different solvent components (30 % water in DES, water, synthetic DES, OxA, and Pro). The number of hydrogen bonds established between water molecules and IMIs was higher compared to those between DES or the components of DES and IMIs (Fig. 4A). In DES, the OxA molecular with two carboxylic acid groups contributed to the formation of hydrogen bonds with IMIs (Fig. 4B). However, the number of hydrogen bonds between IMI and each DES combination was significantly higher than the number between IMI and one water molecule. The hydrogen bond number between each OxA molecular and IMI was 3.3-fold as the number between each water molecular and IMI (Fig. 4C). Thus, the screened DES combination provided abundant hydrogen bonds to fulfill extracting neonicotinoids from beeswax. Considering the potential limitations of molecular dynamics simulations in explaining weak interactions, we employed the GFN2-xTB method combined with the DFT-D4 method to perform the geometry optimization of the DES and IMI clusters. Subsequently, their weak interactions were studied via IGMH analysis. Fig. 4D~E indicated that OxA and Pro in DES can establish robust hydrogen bonds with IMI (highlighted in blue), and the oxygen atom of the carboxylic acid group greatly contributed to the formation of these hydrogen bonds (Fig. 4E). Furthermore, van der Waals forces (Color: green) also contributed to the interaction between DES and IMI, and these results were consistent with previous reports (Liu et al., 2023). In summary, based on the systematic dynamic simulations, the predominant driving forces, which promoted neonicotinoids transferring from beeswax into DES, were confirmed by the contributions of hydrogen bonding and van der Waals forces.

### 3.5. Evaluation of method performance

To validate the method performance, a series of experiments were performed under the optimum conditions, and relevant parameters were evaluated, including linear range, regression coefficient, LOD, LOQ, precision, accuracy, and ME. Calibration curves were established at six levels of each analyte in three parallel experiments, and satisfactory linearities ranging from 0.5 μg/L to 500 μg/L were obtained with acceptable coefficients (R2). LODs and LOQs, measured under the conditions of the signal-to-noise ratios (S/N) of 3 and 10, were in the range of 0.1 to 0.5 μg/mL and 0.4 to 1.0 μg/mL, respectively. The repeated sample analysis and obtained relative standard deviation (RSD, %) was used to express precision. The repeatability and reproducibility of the analytical method were evaluated through repeated sample analysis on the same day and three consecutive days, respectively. The RSDs were determined to be within the range of 4.75 % to 8.9 %, indicating high precision. Trueness was calculated employing recovery experiments. Mean recoveries for neonicotinoid pesticides ranged from 87.4 % to 106.6 %, and RSD values were below 10.9 % (Table S4). ME was

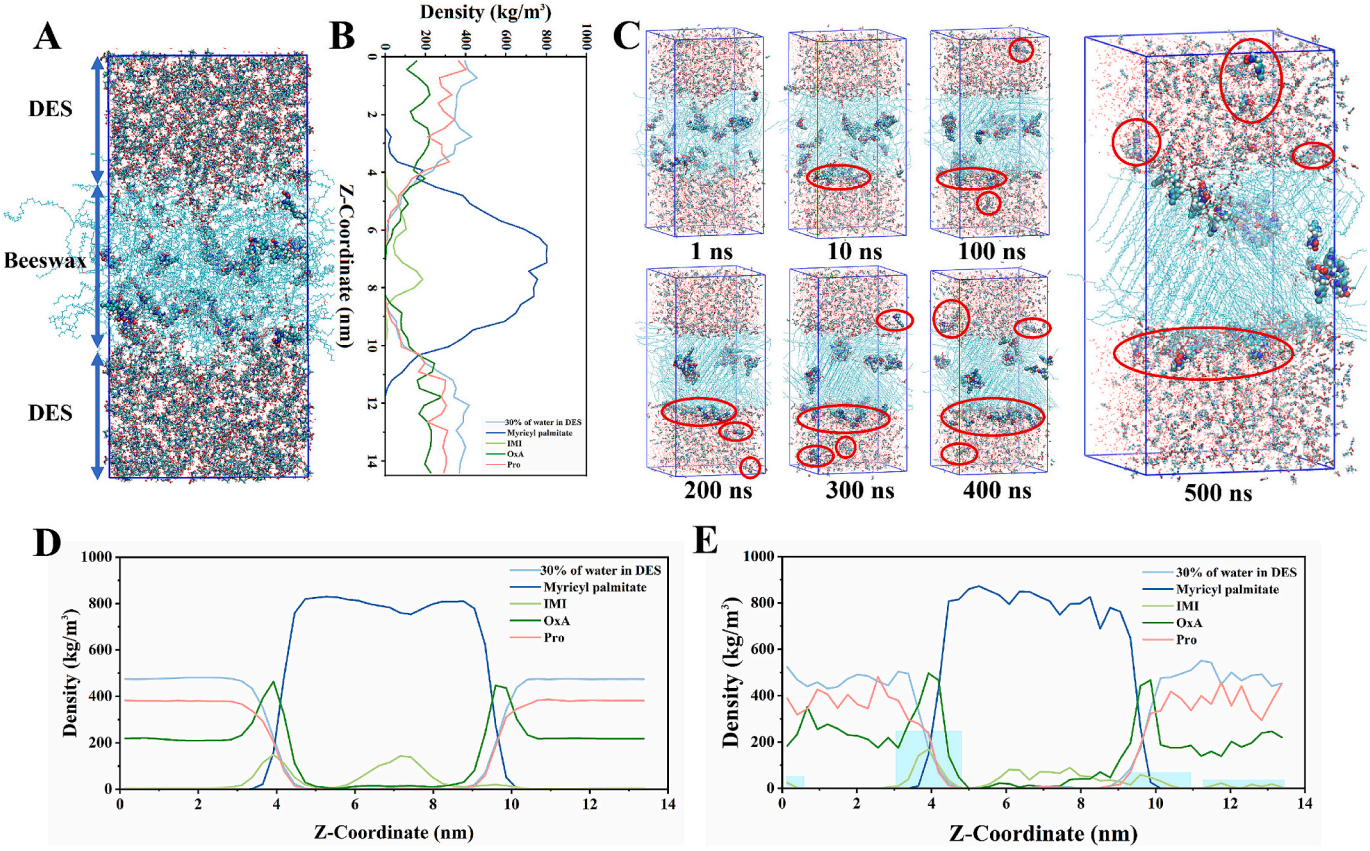


**Fig. 3.** Molecular dynamics simulation results of DES efficient extraction of Imidacloprid from beeswax. (A) The initial system of beeswax-DES two-phase molecular dynamics simulation, (B) The density distribution of different molecules along the *Z*-axis of the initial simulation system, (C) Molecular motion frames under different simulation times, (D) the average density distribution of different molecules in 0–500 ns and (E) the density distribution of different molecules at 500 ns.

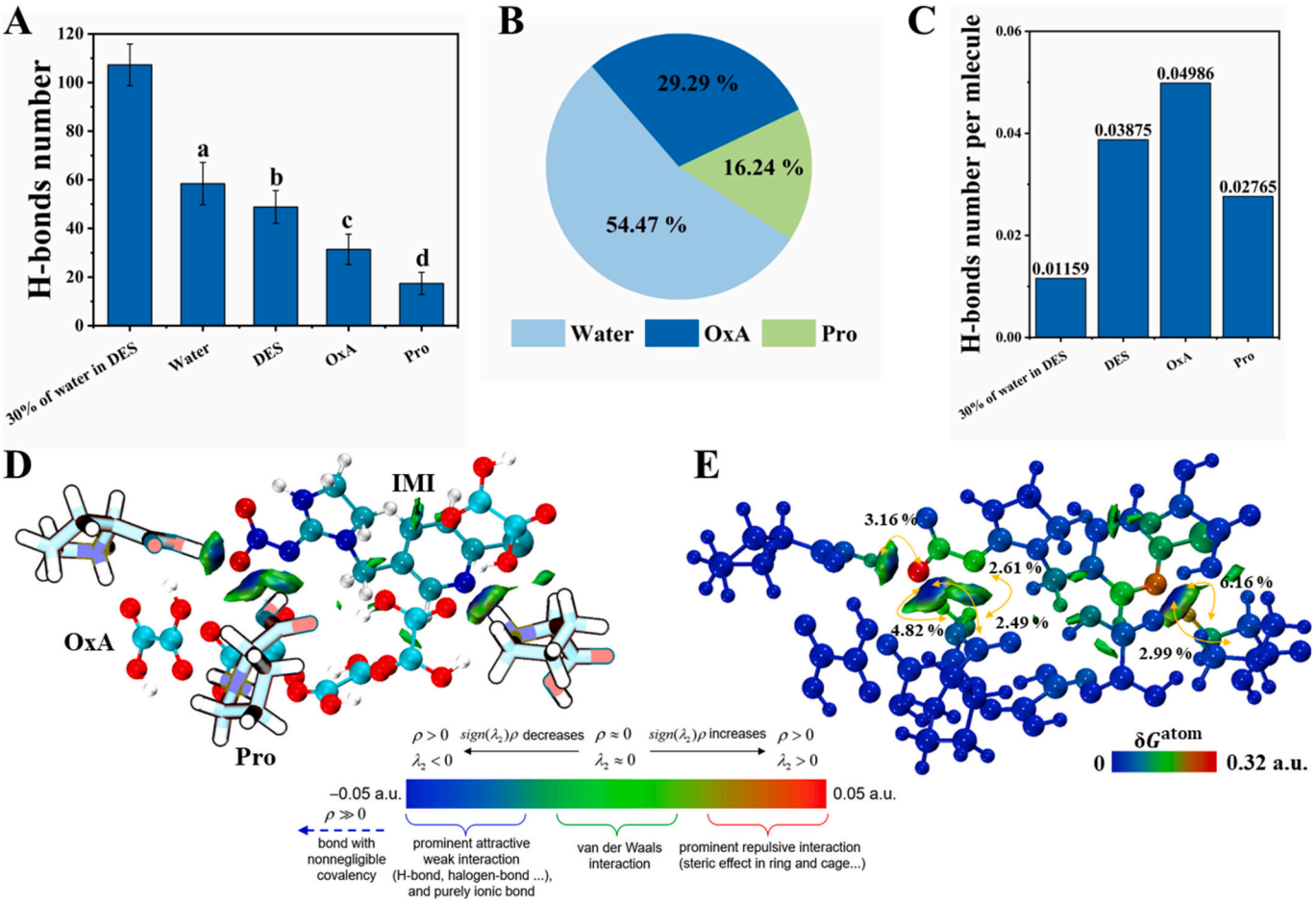


**Fig. 4.** Interaction analysis. (A) The H-bonds number between different solvent molecules and Imidacloprid, (B) H-bond ratio between different solvent molecules and Imidacloprid, (C) The H-bonds number each solvent molecule forms with Imidacloprid, (D) and (E) IGMH and interaction contribution analysis of DES and Imidacloprid clusters optimized by GFN2 method. (Note. In IGMH analysis, the color of the isopotential surface is blue, indicating hydrogen bonding, green represents van der Waals interactions and red represents steric hindrance.) (For interpretation of the references to color in this figure legend, the reader is referred to the web version of this article.)

acquired by comparing the slopes between the matrix-matched calibration curves and the standard calibration curves, when |ME| values in the range from 0 % to 20 % it indicates a weak matrix effect; when |ME| values in the range from 20 % to 50 %, it indicates a medium matrix effect; when |ME| values greater than 50 %, it indicates a strong matrix effect (Zhang et al., 2024). As shown in Table 2, ME values of twelve neonicotinoid pesticides were in the range of −42.57 to 3.61 %. FLO, FLU, SUL, and THI showed a medium matrix effect and the remaining compounds exhibited a weak matrix effect. To compensate for the ME, it is necessary to apply the matrix-matching calibration curve to accurately quantify neonicotinoids in beeswax samples.

### 3.6. Comparison of DES with other extraction methods

Presently, there have been some reports involved in the determination methods of neonicotinoids in beeswax, and we have summarized them in Table 3. The newly developed DES-UHPLC-MS/MS method in this study surpasses traditional approaches by offering an expanded analyte range, improved sensitivity, and significantly enhanced environmental compatibility. Traditional methods typically analyzed fewer

**Table 2**
The method performance of this newly developed method.

| Analytes | Linearity | $R^2$ | LOD | LOQ | Repeatability | Reproducibility | ME |
|---|---|---|---|---|---|---|---|
| | (μg/L) | | (μg/L) | (μg/L) | (RSD%, $n = 6$) | (RSD%, $n = 3$) | (%) |
| ACE | 0.5–500 | 0.9996 | 0.2 | 0.5 | 5.18 | 6.12 | −6.13 |
| CLO | 1–500 | 0.9998 | 0.5 | 1 | 6.35 | 6.31 | −42.57 |
| CYP | 1–500 | 0.9980 | 0.5 | 1 | 4.89 | 5.28 | −14.93 |
| DIN | 1–500 | 0.9986 | 0.5 | 1 | 5.94 | 7.92 | −6.25 |
| FLO | 0.5–500 | 0.9992 | 0.1 | 0.5 | 8.01 | 5.20 | −31.79 |
| FLU | 1–500 | 0.9995 | 0.5 | 1 | 5.81 | 8.86 | −30.02 |
| IMI | 0.5–500 | 0.9998 | 0.1 | 0.3 | 4.97 | 6.44 | −8.12 |
| IMZ | 0.5–500 | 0.9997 | 0.1 | 0.4 | 5.71 | 6.95 | 3.61 |
| NIT | 0.5–500 | 0.9985 | 0.2 | 0.5 | 4.75 | 4.57 | −9.67 |
| SUL | 0.5–500 | 0.9997 | 0.2 | 0.5 | 6.90 | 6.65 | −30.12 |
| THX | 1–500 | 0.9990 | 0.4 | 1 | 6.62 | 4.82 | −12.38 |
| THI | 1–500 | 0.9997 | 0.5 | 1 | 6.90 | 8.90 | −15.32 |

**Table 3**
The comparison of traditional methods with the present approach.

| Analytes | Sample amount | Sample preparation | | | | Analytical performance | | | Ref. |
|---|---|---|---|---|---|---|---|---|---|
| | | Extraction | Clean-up | | Time | Detection | LOD[A] | LOQ[A] | |
| ACE, CLO, IMI, THI and THX | 0.5 g | 4 mL pentane | centrifugation; blow-dry (40 °C) | 2.4 g of diatomaceous earth | ~1 h | LC-MS/MS | 1–5 | 1–20 | (Jabot et al., 2015) |
| ACE, CLO, DIN, IMI, NIT, THI and THX | 1.0 g | 10 mL MeOH-EtOAc (70: 30, v: v) | rotary evaporator (60 °C) | 15mL d-SPE EMR-Lipid tube | ~50 min | LC-Q-TOF | 0.4–1.4 | 1.2–4.9 | (Valverde et al., 2018) |
| ACE, DIN, FLO, FLU, IMI, NIT, THI and THX | 2.0 g | 10 mL H2O, 10 mL ACN | centrifugation (4500 rpm, 5 min) | 4 g anhydrous $MgSO_4$, 1 g $Na_3C_6H_5O_7$.2H2O, 0.5 g $C_6H_6Na_2O_7$.1.5$H_2O$ and 1 g NaCl | overnight | LC-MS/MS | 2 | 5 | (Bommuraj et al., 2019) |
| ACE, CLO, DIN, IMI, NIT, THI and THX | 2.0 g | 15 mL n-hexane-isopropanol (8:2, v: v), 10 mL $H_2O$ | centrifugation (700 rpm, 5 min); rotary evaporator (50 °C) | diatomaceous earth cartridges | / | LC-MS | 0.4–2.6 | 1.5–6.0 | (Karen, José, María, María, & José, 2013) |
| ACE, CLO, CYP, DIN, IMI, NIT, THI and THX | 5.0 g | 10 mL H2O, 10 mL ACN | centrifugation (10,000 rcf, 13 min); rotary evaporator | 4 g anhydrous $MgSO_4$, 1 g $Na_3C_6H_5O_7$.2H2O, 0.5 g $C_6H_6Na_2O_7$.1.5$H_2O$ and 1 g NaCl; 1 g anhydrous $CaCl_2$, 300 mg PSA | ~2 h | LC-MS/MS | 3 | 10 | (El Agrebi et al., 2020) |
| ACE, CLO, DIN, IMI, NIT, THI and THX | 2.0 g | 15 mL n-hexane-isopropanol (8:2, v: v), 10 mL $H_2O$ | centrifugation (700 rpm, 5 min) | diatomaceous earth cartridges | ~1.5 h | CE-MS | 1.0–2.3 | 3.5–7.2 | (Sánchez-Hernández et al., 2014) |
| IMI, THI and THX | 2.0 g | 10 mL ACN | freezer (−18 °C, 2 h); centrifugation (3000 U, 5 min) | 25 mg PSA, 25 mg $C_{18}$ | ~2 h | LC-MS/MS | / | 10 | (Niell et al., 2014) |
| ACE, IMI and THX | 2.0 g | 10 mL ACN | freezer (−18 °C, 2 h); centrifugation (3000 U, 5 min) | 25 mg PSA, 25 mg $C_{18}$ | ~2 h | LC-MS/MS | 0.3 | 1 | (Calatayud-Vernich et al., 2018) |
| ACE, CLO, CYP, DIN, FLO, FLU, IMI, IMZ, NIT, SUL, THI and THX | 5.0 g | 1 mL DES | layering process (75 °C, 2 min) | / | 30 min | UPLC-MS/MS | 0.1–0.5 | 0.4–1.0 | This work |

A: concentration unit: μg/L.

than eight neonicotinoids, whereas this study expanded the compound species up to twelve, providing a more comprehensive residue profile. The optimized DES composition, being guided by molecular dynamics simulations and experimental validation, obtained satisfactory analysis performance. The DES-LLME simplified sample preparation and reduced processing time (< 30 min) while achieving LODs as low as 0.1 μg/L. The detection ability was further confirmed by analyzing neonicotinoid pesticide residues in commercial beeswax and honeycomb beeswax. This work facilitates to control and monitor the quality of apiculture products based on the DES approach. Future applications may extend to real-time monitoring of pesticide residues in other hydrophobic matrixes, improving food and environmental safety.

### *3.7. Actual sample analysis*

The established detection method for neonicotinoid pesticides was applied to analyze real beeswax samples, including thirty honeycomb samples and twenty commercial beeswax samples, and the results are shown in Table S4. ACE and IMI were detected in four positive beeswax samples at measured concentrations in the range of 2.4–18.6 μg/kg, and 2.2–17.0 μg/kg, respectively. THI was detected in one positive beeswax sample at the concentration of 26.4 μg/kg. Presently, there are no standards of the maximum residue limits for neonicotinoid pesticides in beeswax. According to the requirements of plant-derived foodstuffs in China, the No. 22 sample potentially exceeded standards and posed safety worries (Yang et al., 2024). Besides, recovery experiments were performed by spiking different levels (5, 10, and 50 μg/L) to six negative samples. The average recoveries ranged from 87.4 % to 106.6 %, with RSD ranging from 2.1 % to 10.9 %. These results suggested that the established method was available for the determination of neonicotinoid pesticide residues in actual beeswax samples.

## 4. Conclusions

To establish a convenient, simple, quick, and eco,.friendly approach to analyzing neonicotinoids in beeswax, we applied a theoretical design combined with experimental verification to fulfill the development of a novel method. Using COSMO-RS, sixteen potential DES combinations were screened to extract neonicotinoids from beeswax. Verification tests and extraction mechanism simulations determined Pro-OxA as the optimal extraction solvent. Based on this, a DES-LLME combined with UHPLC-MS/MS method was successfully developed for the analysis of neonicotinoids in beeswax. Satisfactory linearities ranged from 0.5 to 500 μg/L with 0.1–0.5 μg/L of LOD and 0.4–1.0 μg/L of LOQ, respectively. Compared to previous methods, this approach can used to simultaneously analyze 12 neonicotinoids with a more simple pre-processing process and less consumption of organic solvents and time. By addressing the challenges of pesticide residue analysis in a super-hydrophobic matrix, our method offers significant advantages over previously established techniques, including a broader analyte range and improved extraction efficiency. It is beneficial for ensuring food safety in apiculture products like beeswax-based coatings and packaging, aiding regulatory compliance and sustainable agriculture. Future work may explore real-time monitoring and applications in other complex matrices, strengthening its role in food safety and environmental protection.

## CRediT authorship contribution statement

**Guodong Mu:** Writing – original draft, Methodology, Investigation, Data curation. **Sha Yan:** Writing – review & editing, Writing – original draft, Investigation, Conceptualization. **Fei Pan:** Methodology, Investigation. **Haitao Xu:** Methodology. **Xu Jing:** Methodology, Conceptualization. **Xiaofeng Xue:** Writing – review & editing, Supervision, Funding

acquisition, Conceptualization.

## Declaration of competing interest

The authors declare that they have no known competing financial interests or personal relationships that could have appeared to influence the work reported in this paper.

## Data availability

No data was used for the research described in the article.

## Acknowledgements

This study was supported by The National Key Research and Development Program of China (2022YFF0607904).

## Appendix A. Supplementary data

Supplementary data to this article can be found online at https://doi.org/10.1016/j.fochx.2024.102073.

## References

Abraham, M. J., Murtola, T., Schulz, R., Páll, S., Smith, J. C., Hess, B., & Lindahl, E. (2015). GROMACS: High performance molecular simulations through multi-level parallelism from laptops to supercomputers. *SoftwareX, 1-2*, 19–25. https://doi.org/10.1016/j.softx.2015.06.001

Bannwarth, C., Caldeweyher, E., Ehlert, S., Hansen, A., Pracht, P., Seibert, J., Spicher, S., & Grimme, S. (2021). Extended tight-binding quantum chemistry methods. *11*(2), Article e1493. https://doi.org/10.1002/wcms.1493

Bannwarth, C., Ehlert, S., & Grimme, S. (2019). GFN2-xTB—An accurate and broadly parametrized self-consistent tight-binding quantum chemical method with multipole electrostatics and density-dependent dispersion contributions. *Journal of Chemical Theory and Computation, 15*(3), 1652–1671. https://doi.org/10.1021/acs.jctc.8b01176

Bento, A. P., Hersey, A., Félix, E., Landrum, G., Gaulton, A., Atkinson, F., … Leach, A. R. (2020). An open source chemical structure curation pipeline using RDKit. *Journal of Cheminformatics, 12*(1), 51. https://doi.org/10.1186/s13321-020-00456-1

Bernardes, R. C., Botina, L. L., Ribas, A., Soares, J. M., & Martins, G. F. (2024). Artificial intelligence-driven tool for spectral analysis: Identifying pesticide contamination in bees from reflectance profiling. *Journal of Hazardous Materials, 480*, Article 136425. https://doi.org/10.1016/j.jhazmat.2024.136425

Bommuraj, V., Chen, Y., Klein, H., Sperling, R., Barel, S., & Shimshoni, J. A. (2019). Pesticide and trace element residues in honey and beeswax combs from Israel in association with human risk assessment and honey adulteration. *Food Chemistry, 299*, Article 125123. https://doi.org/10.1016/j.foodchem.2019.125123

Brito-Pereira, R., Ribeiro, C., Tubio, C. R., Castro, N., Costa, P., & Lanceros-Mendez, S. (2023). Beeswax multifunctional composites with thermal-healing capability and recyclability. *Chemical Engineering Journal, 453*, Article 139840. https://doi.org/10.1016/j.cej.2022.139840

Calatayud-Vernich, P., Calatayud, F., Simó, E., & Picó, Y. (2018). Pesticide residues in honey bees, pollen and beeswax: Assessing beehive exposure. *Environmental Pollution, 241*, 106–114. https://doi.org/10.1016/j.envpol.2018.05.062

Cannavacciuolo, C., Pagliari, S., Celano, R., Campone, L., & Rastrelli, L. (2024). Critical analysis of green extraction techniques used for botanicals: Trends, priorities, and optimization strategies-A review. *TrAC Trends in Analytical Chemistry, 173*, Article 117627. https://doi.org/10.1016/j.trac.2024.117627

Cheng, Y., Zhai, X., Wu, Y., Li, C., Zhang, R., Sun, C., Wang, W., & Hou, H. (2023). Effects of natural wax types on the physicochemical properties of starch/gelatin edible films fabricated by extrusion blowing. *Food Chemistry, 401*, Article 134081. https://doi.org/10.1016/j.foodchem.2022.134081

Cons, B. D., Twigg, D. G., Kumar, R., & Chessari, G. (2022). Electrostatic complementarity in structure-based drug design. *Journal of Medicinal Chemistry, 65*(11), 7476–7488. https://doi.org/10.1021/acs.jmedchem.2c00164

El Agrebi, N., Traynor, K., Wilmart, O., Tosi, S., Leinartz, L., Danneels, E., … Saegerman, C. (2020). Pesticide and veterinary drug residues in Belgian beeswax: Occurrence, toxicity, and risk to honey bees. *Science of the Total Environment, 745*, Article 141036. https://doi.org/10.1016/j.scitotenv.2020.141036

Elik, A., Dogan, B., Demirbas, A., Haq, H. U., Sanaullah, & Altunay, N. (2024). Investigation of use of hydrophilic/hydrophobic NADESs for selective extraction of as (III) and Sb (III) ions in vegetable samples: Air assisted liquid phase microextraction and chemometric optimization. *Food Chemistry, 451*, Article 139538. https://doi.org/10.1016/j.foodchem.2024.139538

Erminia Schiano, M., Sodano, F., Cassiano, C., Magli, E., Seccia, S., Grazia Rimoli, M., & Albrizio, S. (2024). Monitoring of seven pesticide residues by LC-MS/MS in extra virgin olive oil samples and risk assessment for consumers. *Food Chemistry, 442*, Article 138498. https://doi.org/10.1016/j.foodchem.2024.138498

Gao, Y., Lei, Y., Wu, Y., Liang, H., Li, J., Pei, Y., Li, Y., Li, B., Luo, X., & Liu, S. (2021). Beeswax: A potential self-emulsifying agent for the construction of thermal-sensitive food W/O emulsion. *Food Chemistry, 349*, Article 129203. https://doi.org/10.1016/j.foodchem.2021.129203

Giampieri, F., Quiles, J. L., Cianciosi, D., Forbes-Hernández, T. Y., Orantes-Bermejo, F. J., Alvarez-Suarez, J. M., & Battino, M. (2022). Bee products: An emblematic example of underutilized sources of bioactive compounds. *Journal of Agricultural and Food Chemistry, 70*(23), 6833–6844. https://doi.org/10.1021/acs.jafc.1c05822

Gutiérrez, A., Atilhan, M., & Aparicio, S. (2021). Molecular dynamics study on water confinement in deep eutectic solvents. *Journal of Molecular Liquids, 339*, Article 116758. https://doi.org/10.1016/j.molliq.2021.116758

Hanwell, M. D., Curtis, D. E., Lonie, D. C., Vandermeersch, T., Zurek, E., & Hutchison, G. R. (2012). Avogadro: An advanced semantic chemical editor, visualization, and analysis platform. *Journal of Cheminformatics, 4*(1), 17. https://doi.org/10.1186/1758-2946-4-17

Hosseini, S. F., Mousavi, Z., & McClements, D. J. (2023). Beeswax: A review on the recent progress in the development of superhydrophobic films/coatings and their applications in fruits preservation. *Food Chemistry, 424*, Article 136404. https://doi.org/10.1016/j.foodchem.2023.136404

Huang, Y., Feng, F., Jiang, J., Qiao, Y., Wu, T., Voglmeir, J., & Chen, Z.-G. (2017). Green and efficient extraction of rutin from tartary buckwheat hull by using natural deep eutectic solvents. *Food Chemistry, 221*, 1400–1405. https://doi.org/10.1016/j.foodchem.2016.11.013

Jabot, C., Fieu, M., Giroud, B., Buleté, A., Casabianca, H., & Vulliet, E. (2015). Trace-level determination of pyrethroid, neonicotinoid and carboxamide pesticides in beeswax using dispersive solid-phase extraction followed by ultra-high-performance liquid chromatography-tandem mass spectrometry. *International Journal of Environmental Analytical Chemistry, 95*(3), 240–257. https://doi.org/10.1080/03067319.2015.1016011

Ju, Z. W., Fan, J. X., Meng, Z. L., Lu, R. H., Gao, H. X., & Zhou, W. F. (2023). A high-throughput semi-automated dispersive liquid-liquid microextraction based on deep eutectic solvent for the determination of neonicotinoid pesticides in edible oils. *Microchemical Journal, 185*, Article 108193. https://doi.org/10.1016/j.microc.2022.108193

Karen, P. Y., José, L. B., María, J. N., María, T. M., & José, B. (2013). Determination of seven neonicotinoid insecticides in beeswax by liquid chromatography coupled to electrospray-mass spectrometry using a fused-core column. *Journal of Chromatography A, 1285*, 110–117. https://doi.org/10.1016/j.chroma.2013.02.032

Lefebvre, C., Rubez, G., Khartabil, H., Boisson, J.-C., Contreras-García, J., & Hénon, E. (2017). Accurately extracting the signature of intermolecular interactions present in the NCI plot of the reduced density gradient versus electron density. *Physical Chemistry Chemical Physics, 19*(27), 17928–17936. https://doi.org/10.1039/C7CP02110K

Liu, Y., Zhang, S., Lou, L., Yan, T., & Xu, W. (2023). Evaluating the behavior and principle of deep eutectic solvent on ephedrine-type alkaloid extraction from Ephedrae Herba. *Biomedical Chromatography, 37*(2), Article e5541. https://doi.org/10.1002/bmc.5541

Lozano, A., Hernando, M. D., Uclés, S., Hakme, E., & Fernández-Alba, A. R. (2019). Identification and measurement of veterinary drug residues in beehive products. *Food Chemistry, 274*, 61–70. https://doi.org/10.1016/j.foodchem.2018.08.055

Lu, T., & Chen, F. (2012). Multiwfn: A multifunctional wavefunction analyzer. *Journal of Computational Chemistry, 33*(5), 580–592. https://doi.org/10.1002/jcc.22885

Maggiora, G. M. (2014). Introduction to molecular similarity and chemical space. In K. Martinez-Mayorga, & J. L. Medina-Franco (Eds.), *Foodinformatics: Applications of chemical information to food chemistry* (pp. 1–81). Cham: Springer International Publishing. https://doi.org/10.1007/978-3-319-10226-9_1.

Maia, M., & Nunes, F. M. (2013). Authentication of beeswax (*Apis mellifera*) by high-temperature gas chromatography and chemometric analysis. *Food Chemistry, 136*(2), 961–968. https://doi.org/10.1016/j.foodchem.2012.09.003

Murcia-Morales, M., Heinzen, H., Parrilla-Vázquez, P., Gómez-Ramos, M. D. M., & Fernández-Alba, A. R. (2022). Presence and distribution of pesticides in apicultural products: A critical appraisal. *TrAC Trends in Analytical Chemistry, 146*, Article 116506. https://doi.org/10.1016/j.trac.2021.116506

Neese, F. (2018). Software update: The ORCA program system, version 4.0. *WIREs Computational Molecular Science, 8*, Article e1327. https://doi.org/10.1002/wcms.1327

Niell, S., Cesio, V., Hepperle, J., Doerk, D., Kirsch, L., Kolberg, D., Scherbaum, E., Anastassiades, M., & Heinzen, H. (2014). QuEChERS-based method for the multiresidue analysis of pesticides in beeswax by LC-MS/MS and GC×GC-TOF. *Journal of Agricultural and Food Chemistry, 62*(17), 3675–3683. https://doi.org/10.1021/jf405771t

Pan, F., Li, X., Tuersuntuoheti, T., Wang, W., Zheng, X., Fang, X., Tian, W., & Peng, W. (2023). Molecular mechanism of high-pressure processing regulates the aggregation of major royal jelly proteins. *Food Hydrocolloids, 144*, Article 108928. https://doi.org/10.1016/j.foodhyd.2023.108928

Politzer, P., & Murray, J. S. (2021). Molecular electrostatic potentials: Significance and applications. In P. K. Chattaraj, & D. Chakraborty (Eds.), *Chemical reactivity in confined systems*. https://doi.org/10.1002/9781119683353.ch7

Sánchez-Hernández, L., Hernández-Domínguez, D., Bernal, J., Neusüß, C., Martín, M. T., & Bernal, J. L. (2014). Capillary electrophoresis–mass spectrometry as a new approach to analyze neonicotinoid insecticides. *Journal of Chromatography A, 1359*, 317–324. https://doi.org/10.1016/j.chroma.2014.07.028

Sapir, L., & Harries, D. (2020). Restructuring a deep eutectic solvent by water: The nanostructure of hydrated choline chloride/urea. *Journal of Chemical Theory and Computation, 16*(5), 3335–3342. https://doi.org/10.1021/acs.jctc.0c00120

Silvina, N., Florencia, J., Nicolás, P., Cecilia, P., Lucía, P., Abbate, S., … Horacio, H. (2017). Neonicotinoids transference from the field to the hive by honey bees: Towards a pesticide residues biomonitor. *Science of the Total Environment, 581*, 25–31. https://doi.org/10.1016/j.scitotenv.2017.01.011

Tesfaye, B., Gure, A., Asere, T. G., & Molole, G. J. (2023). Deep eutectic solvent-based dispersive liquid-liquid microextraction for determination of organochlorine pesticides in water and apple juice samples. *Microchemical Journal, 195*, Article 109428. https://doi.org/10.1016/j.microc.2023.109428

Tu, X., Du, C., He, Y., Yang, J., Chen, J., Jin, Q., Xie, L., Zuo, Y., Huang, S., & Chen, W. (2024). Determination of bisphenols in beeswax based on sugaring out–assisted liquid–liquid extraction: Method development and application in survey, recycling and degradation studies. *Chemosphere, 351*, Article 141274. https://doi.org/10.1016/j.chemosphere.2024.141274

Tu, X. J., & Chen, W. B. (2021). Overview of analytical methods for the determination of neonicotinoid pesticides in honeybee products and honeybee. *Critical Reviews in Analytical Chemistry, 51*(4), 329–338. https://doi.org/10.1080/10408347.2020.1728516

Valverde, S., Ares, A. M., Bernal, J. L., Nozal, M. J., & Bernal, J. (2018). Fast determination of neonicotinoid insecticides in beeswax by ultra-high performance liquid chromatography-tandem mass spectrometry using an enhanced matrix removal-lipid sorbent for clean-up. *Microchemical Journal, 142*, 70–77. https://doi.org/10.1016/j.microc.2018.06.020

Wang, D., Zhang, M., Law, C. L., & Zhang, L. (2024). Natural deep eutectic solvents for the extraction of lentinan from shiitake mushroom: COSMO-RS screening and ANN-GA optimizing conditions. *Food Chemistry, 430*, Article 136990. https://doi.org/10.1016/j.foodchem.2023.136990

Wang, Z., Wang, D., Fang, J., Song, Z., Geng, J., Zhao, J., Fang, Y., Wang, C., & Li, M. (2024). Green and efficient extraction of flavonoids from *Perilla frutescens* (L.) Britt. Leaves based on natural deep eutectic solvents: Process optimization, component identification, and biological activity. *Food Chemistry, 452*, Article 139508. https://doi.org/10.1016/j.foodchem.2024.139508

Wojeicchowski, J. P., Ferreira, A. M., Abranches, D. O., Mafra, M. R., & Coutinho, J. A. P. (2020). Using COSMO-RS in the Design of Deep Eutectic Solvents for the extraction of antioxidants from rosemary. *ACS Sustainable Chemistry & Engineering, 8*(32), 12132–12141. https://doi.org/10.1021/acssuschemeng.0c03553

Xu, H., Lin, J., Liu, Q., Chen, Y., Zhang, J., Yang, Y., … Mo, F. (2022). High-throughput discovery of chemical structure-polarity relationships combining automation and machine-learning techniques. *Chem, 8*(12), 3202–3214. https://doi.org/10.1016/j.chempr.2022.08.008

Yáñez, K. P., Bernal, J. L., Nozal, M. J., Martín, M. T., & Bernal, J. (2013a). Determination of seven neonicotinoid insecticides in beeswax by liquid chromatography coupled to electrospray-mass spectrometry using a fused-core column. *Journal of Chromatography A, 1285*, 110–117. https://doi.org/10.1016/j.chroma.2013.02.032

Yáñez, K. P., Bernal, J. L., Nozal, M. J., Martín, M. T., & Bernal, J. (2013b). Fast determination of Imidacloprid in beeswax by liquid chromatography coupled to electrospray-mass spectrometry. *Current Analytical Chemistry, 9*(3), 495–503. https://doi.org/10.2174/1573411011309030019

Yang, B., Tu, M., Wang, S., Ma, W., Zhu, Y., Ma, Z., & Li, X. (2024). Neonicotinoid insecticides in plant-derived foodstuffs: A review of separation and determination methods based on liquid chromatography. *Food Chemistry, 444*, Article 138695. https://doi.org/10.1016/j.foodchem.2024.138695

Yang, J., Cai, Y., Zhao, K., Xie, H., & Chen, X. (2022). Concepts and applications of chemical fingerprint for hit and lead screening. *Drug Discovery Today, 27*(11), Article 103356. https://doi.org/10.1016/j.drudis.2022.103356

Zhang, W., Zhou, C., Zhou, F., Zalán, Z., Shi, H., Kan, J., Cai, T., & Chen, K. (2024). Determination of twelve neonicotinoid pesticides in chili using an improved QuEChERS method with UPLC-Q-TOF/MS. *Food Chemistry, 452*, Article 139463. https://doi.org/10.1016/j.foodchem.2024.139463